Design, Synthesis, and Cytoprotective Effect of 2-Aminothiazole Analogues as Potent Poly(ADP-Ribose) Polymerase-1 Inhibitors

Wen-Ting Zhang,[†] Jin-Lan Ruan,[†,§] Peng-Fei Wu,[‡] Feng-Chao Jiang,*,[†,§] Li–Na Zhang,[†] Wei Fang,[†] Xiang-Long Chen,[‡] Yue Wang,[†] Bao-Shuai Cao,[†] Gang-Ying Chen,[†] Yi-Jing Zhu,[†] Jun Gu,[‡] and Jian-Guo Chen*,[‡,§]

Department of Medicinal Chemistry and Department of Pharmacology, Tongji Medical College, Huazhong University of Science and Technology, The Key Laboratory of Natural Medicinal Chemistry and Resource Evaluation of Hubei Province, 13 Hangkong Road, Wuhan 430030, China

A series of novel poly(ADP-ribose) polymerase-1 (PARP-1) inhibitors were designed within 2-aminothiazole analogues (**4−10**) based on a constructed three-dimensional pharmacophore model. After synthesis, the inhibitory effect on PARP-1 activity and the cytoprotective action of these compounds were tested and evaluated. Among them, compounds **4−6** and **10** appeared to be potent PARP-1 inhibitors with IC_{50} values less than 1 μM, which had been perfectly predicted by pharmacophore model. These compounds proved to be highly potent against cell injury induced by H_2O_2 and oxygen-glucose deprivation (OGD) in PC12 cells. These novel 2-aminothiazole analogues are potentially applicable as neuroprotective agents for the treatment of neurological diseases.

Introduction

Poly(ADP-ribose) polymerase (PARP[a]) is known as a nuclear enzyme that catalyzes poly(ADP-ribosyl)ation of DNA-binding proteins, regulates the immediate cellular response to DNA damage, and facilitates DNA repair.[1] Eighteen different putative PARP homologues were found, and at least seven members of the PARP family were characterized to various degrees so far (PARP-1−3, PARP-4 (VPARP), PARP-5a (tankyrase 1), PARP-5b (tankyrase 2), PARP-7 (TiPARP)).[2] PARP-1 is regarded as the best characterized member of the PARP family, which is a 116 kDa nuclear protein composed of four main regions: an N-terminal DNA binding domain with two zinc finger motifs, a nuclear location signal containing a caspase-3 cleavage site, an automodification domain, and a C-terminal catalytic domain.[3] It is activated in response to DNA damage such as that induced by DNA-binding agents, radiation, or oxidative stress. When the DNA damage is moderate, PARP-1 participates in the DNA repair process. Conversely, in the case of massive and unrepairable DNA injury, overactivation of PARP-1 can lead to necrotic cell death caused by the depletion of NAD^+ and ATP.[4] Besides that, PARP-1 is involved in the regulation of inflammatory mediators and in the development of LPS-induced endotoxic shock.[5] PARP-1 is also associated with NMDA-mediated excitotoxicity and myocardial postichemic injury.[6,7] Recent findings suggest that extensive PARP-1 activation may also result in caspase-independent programmed cell death, mediated by the translocation of apoptosis-inducing factor (AIF) from the mitochondria to the nucleus.[8]

Because of its role in many common pathologies of various central nervous system (CNS) diseases such as cell death, inflammatory responses, excitotoxicity, and mitochondria functional disorder, PARP-1 has attracted more and more attention as a suitable target for neuroprotective agents.[9] Extensive investigations have been conducted in the identification of novel PARP-1 inhibitors. Most of the PARP-1 inhibitors so far developed are structural analogues of NAD^+ and compete with NAD^+ at the level of the catalytic domain. Early PARP-1 inhibitors were benzamide derivatives, which characterized by low potency and poor selectivity. Subsequently, there are various compounds reported as PARP-1 inhibitors, including imidazobenzodiazepines,[10] quinazolinone and quinoxaline derivatives,[11] substituted uracil derivatives,[12] adenosine substituted isoindolones,[13] phthalazinones,[14] phenanthridin-6-ones,[15] and naphthyridin-6-ones.[16] Although some of these PARP-1inhibitors displayed potent in vitro activity, they lacked specificity and had poor physical properties, complicated synthesis, or in vivo side effects. In this study, we devote ourselves to explore novel PARP-1 inhibitors. Herein, a series of compounds with 2-aminothiazole framework have been schemed out via computer-aided drug design.

Design

The hypothesis generation methods (HipHop and HypoGen) of the Catalyst software have been successfully used in drug discovery research. The Catalyst generated pharmacophores can be considered as the ensemble of steric and electrostatic features of different compounds and effectively used for rational drug design.[17−20] In our previous research, the pharmacophore model of PARP-1 inhibitors had been developed by HypoGen process in Catalyst system, which can correlate the observed biological activities of a series of compounds with their corresponding structures. A training set consisting of 38 compounds with seven different classes of diverse structures and high activity was selected in order to improve the applicability and universality of the pharmacophore model.[10−16] The selected range of IC_{50}

* To whom correspondence should be addressed. For F.-C.J.: phone, (86)-027-83692749; fax, (86)-027-83692749; E-mail, fengchao@mails.tjmu.edu.cn. For J.-G.C.: phone, (86)-027-83692628; fax, (86)-027-83692847; E-mail, chenj@mails.tjmu.edu.cn.

† Department of Medicinal Chemistry, Tongji Medical College, Huazhong University of Science and Technology.

‡ Department of Pharmacology, Tongji Medical College, Huazhong University of Science and Technology.

§ The Key Laboratory of Natural Medicinal Chemistry and Resource Evaluation of Hubei Province.

a Abbreviations: PARP, poly(ADP-ribose) polymerase; OGD, oxygen-glucose deprivation; AIF, apoptosis-inducing factor; CNS, central nervous system; HA, hydrogen bond acceptor; HPAR, hydrophobic aromatic; HD, hydrogen bond donor; TPSA, total polar surface area; DCC, *N,N*-dicyclohexylcarbodiimide; DMAP, 4-dimethylaminopyridine; 3-AB, 3-aminobenzaminde; FITC, fluorescein isothiocyanate; PI, propidium iodide; HRP, horseradish-peroxidase.

values varied from 3.8 to 770 nM. The training set of compounds was dealt with by generating molecular model, making conformational analysis and generating hypothesis. Ten models were obtained after automatic construction, and the best pharmacophore in terms of statistics and predictive value consisted of four features: two hydrogen bond acceptors (HA units) and two hydrophobic aromatic cores (HPAR units). It was selected with the lowest error cost, lowest rms difference, and the best correlation coefficient (Weight = 2.1, rms = 0.46, Correl = 0.91, Config = 15.97) from mapping of the training set. Each unit met the special limitation in distance. As can be seen in Figure 1, the activities of training set compounds was perfectly predicted by the model (r = 0.91). The pharmacophore model had also been validated on 12 highly active test inhibitors such as imidazobenzodiazepines, quinazolinone and quinoxaline derivatives, phthalazinones, phenanthridin-6-ones, and naphthyridin-6-ones.[21] Besides that, it is well-known that most PARP-1 inhibitors have been designed to bind at the position of the nicotiamide subsite of the NAD$^+$ binding pocket. Generally, inhibitors interact with Gly863 and Ser904 by the hydrogen bonds, with Tyr896 and Tyr907 forming the walls of the nicotinamide-binding pocket by hydrophobic interaction.[22] The docking and QSAR analysis have demonstrated that the amide moiety of the inhibitor invariably interacted with Gly863, while the aromatic portion interacted possibly through $\pi-\pi$ interactions, and the extension of the contact surfaces between inhibitors and enzyme was in favor of high inhibitory potency.[23] Similarly, the pharmacophore model built in our experiment also indicated that HA and HPAR interactions were the most important elements that affected the inhibitory action of compounds. Accordingly, the model which has good applicability and forecast ability can be a guidance for discovering novel PARP-1 inhibitors.

On the basis of the constructed pharmacophore model, we screened the library to find structures fitting this model. We found that aminothiazoles have almost ubiquitous presence in pharmaceutical test samples and have been used as attractive candidates for treatment of CNS disorders. They have extensive biological activity and possess fine stability and little side effects. For example, 2-aminothiazole schiff base compounds have been designed for cognition enhancers,[24] and 2,6-diaminotetrahydrobenzothiazole analogue has shown a pronounced selectivity for DA autoreceptors.[25] The potential radical-scavenging ability of 2-aminothiazole amide compounds was also known,[26] and 2-aminothiazole analogue has been used as the lead compound to explore novel p53 inactivators with neuroprotective effect.[27] As a result, molecules with 2-aminothiazole framework were chosen as a scaffold for further chemical modification to explore potent PARP-1 inhibitors with neuroprotection (**1−3**). The
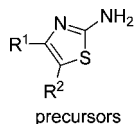
1: R^1= phenyl-; R^2= -H
2: R^1, R^2= -CH$_2$CH$_2$CH$_2$CH$_2$-
3: R^1= 2,4-diethoxyphenyl-; R^2= -H

precursors

candidates with this framework were designed and screened out. A 3D conformation with minimum energy was generated and displayed based on the current 3D structure for each compound. After conformational analysis, each molecule got a group of conformations reasonable in energy using the "best quality" process. Then View Hypothesis Workbench helped to map each molecule onto the pharmacophoric units and compare the fit in order to test the inosculated degree of pharmacophore model with the specific conformation of the related compound. Besides, CNS-penetrant compounds should possess appropriate properties

Table 1. The Matching with Pharmacophore Model and Calculated Physicochemical Properties for Designed Compounds and **3-AB**

compd.	R^1	Fit [a]	TPSA [b]	MW [b]	logP [b]	HD [b]	HA [b]
4	-CH$_2$CH$_2$COOC$_2$H$_5$	5.6	68	304	3.3	1	5
5	-4-pyridyl	5.3	55	281	2.9	1	4
6	-styryl	5.5	42	306	4.7	1	3
7	-3,5-dimethoxystyryl	5.7	60	366	4.7	1	5
8	-CH$_2$CH$_2$COOC$_2$H$_5$	5.0	68	282	2.2	1	5
9	-3,5-dimethoxystyryl	5.7	60	344	3.6	1	5
10		5.3	59	391	6.1	1	5
3-AB		4.1	69	136	0.1	2	3

[a] The inosculated degree of pharmacophore model with the specific conformation of the related compounds. [b] Physicochemical properties were calculated using Pallas 3.3 software.

such as size, lipophilicity, hydrongen-bonding potential, charge, and conformation. Herein, our approach to design novel PARP-1 inhibitors was based on the premise that they could match the pharmacophore model and possess appropriate physical properties. The following criteria used for design:

(1) Compound was selected if the value of fit was more than 5.

(2) The estimated value of bioavailability for selected compound accorded with the rule of 5.

(3) If estimated value of total polar surface area (TPSA) for a compound was more than 90 Å, then it was deselected.

Only simple structures and several representatives of a certain chemical series were selected. Finally, seven 2-aminothiazole analogues (**4−10**) were selected and their activities of PARP-1 inhibition were predicted by pharmacophore. However, so far as we are aware, there are no publications concerning the PARP-1 inhibition in compounds from these chemical series. As can be seen in Figure 2, the designed compounds successfully mapped on all or at least three features of the selected pharmacophore developed against PARP-1, whereas 3-aminobenzamide (**3-AB**) only could map two features of it. And the predicted physicochemical properties of these compounds indicated that they possess good lipophilicity and CNS-penetrant effect. The structures, values of fit, and calculated physicochemical properties of these compounds were shown in Table 1. Then they were synthesized and experimentally tested as cytoprotective agents.

Chemistry

In this study, we prepared 2-aminothiazole analogues in which the application of microwave technology was used for cyclization reaction. As shown in Scheme 1, the synthesis of 4,5-substituted-2- aminothiazole (**1−3**) was according to a published procedure.[28,29] The cyclization step, carried by microwave, was performed in only a few minutes compared to the conventional thermal heating for 12 h. The crude product from the reaction of commercially available acetophenone or cyclohexanone with thiourea in the presence of iodine was extracted with ether, dissolved in boiling water, and made basic with solid Na$_2$CO$_3$ to give compound **1−3** as crystal.

Table 2. Inhibitory Effect on PARP-1 Activity (IC_{50}) and Cytoprotective Activity (EC_{50}) of 2-Aminothiazole Analogues

compd	IC_{50}[a]	IC_{50}[b]	error[c]	$E_{conform}$[d]	EC_{50}[e]	EC_{50}[f]
4	140	240	1.7	38.47	537	143
5	260	753	2.9	25.45	1548	191
6	150	224	1.5	13.86	129	559
7	92	4533	49.3	65.49	1122	527
8	580	12399	21.4	59.72	>3000	961
9	88	9332	106.0	67.62	2089	1036
10	220	682	3.1	22.94	324	361
3-AB	4000	9005	2.2	0		

[a] Estimated IC_{50} values (nM) were predicted by Catalyst software. [b] Experimental IC_{50} values (nM) were determined from logit plots of inhibition% vs compound concentration and were calculated from mean values at 3−5 concentrations (in each, correlation coefficients r^2 >0.9). [c] error = IC_{50} (experimental)/IC_{50} (estimated). [d] $E_{conform}$ (kJ·mol^{-1}) represents the potential energy of the structure bearing the alignment with the pharmacophore model. [e] Concentration of compounds required to induce 50% protection of PC12 cells from H_2O_2-induced cell death (EC_{50}, nM). [f] Concentration of compounds required to induce 50% protection of PC12 cells from OGD-induced cell death (EC_{50}, nM).

Compound **1** or **2** was stirred with acid or acyl chloride, respectively. They were shaken in acetone at room temperature for 24 h, extracted with acetone, and volatilized to give the crude compound **4−9**, which were recrystallized from alcohol to afford compound **4−9** as crystal. Compound **3** reacted with aldehyde in ethanol at 80−90 °C for two days and extracted with ether to give the crude compound, which were recrystallized from EtOH/Et$_2$O to afford compound **10** as crystal, and the reaction time was shortened from two days to 1 h by microwave.

Biological Results and Discussion

Assay for PARP-1 Inhibition in Vitro. The inhibitory effect of these compounds on PARP-1 activity was summarized in Table 2. The prototypical PARP-1 inhibitor, **3-AB**, inhibited the activity of PARP at a wide range of concentrations from 2 μM to 10 mM. The IC_{50} value of **3-AB** was 9005 nM under the same experimental conditions. As shown in Figure 3, compounds **4−6** and **10** almost showed more than 50% PARP-1 inhibition at a concentration of 1 μM. Parenthetically, the compounds **4−6** and **10** possess a 4-phenyl moiety and were more potent (IC_{50} 240, 753, 224, and 682 nM, respectively). Analogue **4** has a 4-phenyl moiety and was more potent than the analogous compound **8**, which possesses a 4-(4′, 5′, 6′, 7′-tetrahydrobenzo) moiety (IC_{50} > 10 μM). As exemplified above, compounds with 4-phenyl group showed a large increase in inhibitory activity.

As shown in Table 2, the experimental IC_{50} values of compounds **4−6**, **10**, and **3-AB** were closed to their estimated values, while compounds **7−9** were on the contrary. And the corresponding potential energies of them bearing the alignment with pharmacophore model were lower than those of compounds **7−9**. It is well-known that when a receptor recognizes and acts with a ligand, the conformation of this ligand will change to some extent according to the induced fit theory and the energy of this conformer may be even higher than that of the minimum energy conformer. An allowable energy interval between an active conformer ($E_{conform} \geq 0$) and the minimum energy conformer ($E_{conform} = 0$) is maintained within a certain limit. The system default value of the limit is 84 kJ·mol^{-1} in the process of conformational analysis by Catalyst. It is obvious that molecules with lower active conformation energy are prone to approach the enzyme and bind with it. In actual environment, when a compound acts with PARP-1 with the theoretically active conformer calculated by pharmacophore model, it must conquer the energy interval and leads to system instability, which is

responsible for the difference between estimated activity and actual activity. Thus, the reason why the error values of compounds **7−9** were greater is not the inaccuracy of the pharmacophore model but the greater $E_{conform}$ values of them to a great extent, although the values were within 84 kJ·mol^{-1}. Obviously, the inhibitory activity of **3-AB** was accurately predicted in despite of a low potency because its active conformer was just the minimum energy conformer ($E_{conform} = 0$). So the pharmacophore model is creditable and we should pay more attention to $E_{conform}$ values of compounds in further design study.

Assays for Cytoprotective Action in PC12 Cells. The oxidative stress may induce DNA damage and PARP-1 activation. First, the cytoprotective effects of these novel PARP-1 inhibitors against oxidant-induced cell death were tested with an H_2O_2-induced PC12 cell injury model. In MTT assay, compounds **6** and **10** were highly protective (EC_{50} 129 and 324 nM, respectively, Table 2) and compounds **4**, **5**, and **7** were moderately protective. Because inhibition of PARP-1 activity have been shown to help prevent ischemic injury in the brain,[30] we also generated an oxygen-glucose deprivation (OGD) induced PC12 cell death model to evaluate the efficacy of these compounds in the treatment of acute ischemic insults. As can be seen in Figure 5A, compounds **4**, **5**, and **10** were more protective (EC_{50} 143, 191, and 361 nM, respectively, Table 2) in MTT assay. Anyway, within the same cell, the common biochemical pathway leading to cell death via PARP-1 can be differentially stimulated by different DNA damage insults with divergent pharmacological targets. In addition, when the IC_{50} values observed in the PARP-1 activity assay for these compounds were compared with their EC_{50} values for the reduction of H_2O_2-induced or OGD-induced cell death, a significant correlation was found ($r = 0.90$, $P < 0.0053$, Figure 4B; $r = 0.89$, $P < 0.0072$, Figure 5B). Apparently, the compounds possessing better PARP-1 inhibition showed better cytoprotective activity in protecting PC12 cells exposed to H_2O_2 or OGD treatment. To a certain extent, a 50% effective concentration for cytoprotection was commensurate with the inhibition of PARP-1, although some extracellular cytoprotective effects may act at the same time.

To confirm the cytoprotective effect of 2-aminothiazole analogues, another experiment of measuring cell viability with LDH release assay was performed after OGD treatment in PC12 cells. It has been previously established that LDH release correlates linearly with the number of damaged cells after toxic insult. In LDH assay, compounds **4−7** and **10** (3 μM) significantly reduced the OGD-induced LDH release by 34.6%, 20.1%, 33.1%, 24.0%, and 28.4%, respectively (Figure 6). We also performed a biparametric cytofluorimetric analysis using fluorescein isothiocyanate (FITC)-conjugated annexin V and propidium iodide (PI) double staining. Annexin V has been utilized to detect the externalization of phosphatidylserine that occurs at an early stage of apoptosis and PI was used as a marker of necrosis due to cell membrane destruction. The distribution of stained cells was shown in Figure 7. A concentration of 3 μM of compounds **4−6** significantly reduced OGD-induced total apoptotic cells (early and late apoptotic cells) by 70.7%, 45.1%, and 64.4%, respectively and exhibited a considerable protective effect on OGD-induced PC12 cell damage, which indicated the cytoprotective activity of potent PARP-1 inhibitors were relevant to their antiapoptotic effect to some extent.

Conclusion

We described herein a novel series of potent PARP-1 inhibitors with cytoprotective activity designed by pharmacor-

Scheme 1. Synthesis of Compounds **1**−**10**[a]
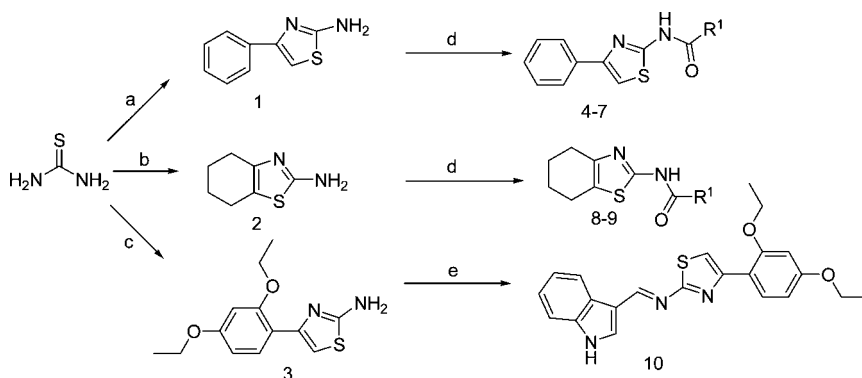
[a] Reagents and conditions: (a) acetophenone, iodine, microwave (130W-65W), Na$_2$CO$_3$; (b) cyclohexanone, iodine, microwave (130W-65W), Na$_2$CO$_3$; (c) 1-(2,4-diethoxyphenyl)ethanone, iodine, microwave (130W-65W), Na$_2$CO$_3$; (d) aromatic acid or acyl chloride, DMAP or DCC, acetone, rt; (e) 1*H*-indole-3-carbaldehyde, dehydrated alcohol, piperidine, microwave (65W-130W).
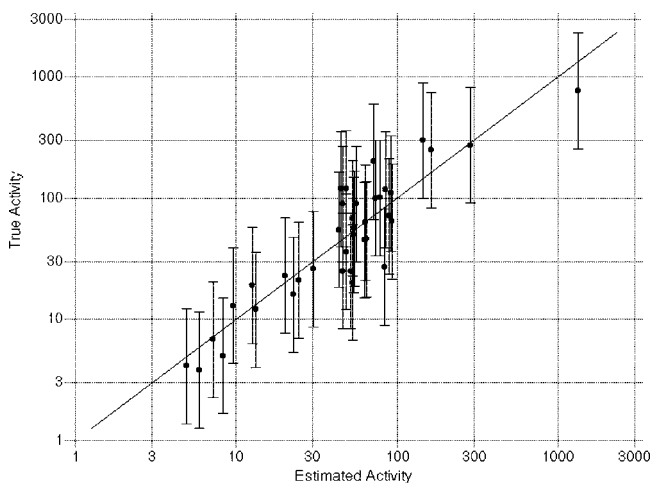

Figure 1. Correlation line of estimated activity vs actual activity for the 38 training compounds from refs 10−16 including imidazobenzo-diazepines, quinazolinone and quinoxaline derivatives, substituted uracil derivatives, phenanthridin-6-ones, adenosine substituted 2,3-dihydro-1*H*-isoindol-1-ones, and phthalazinones ($r = 0.91$).[21]

phore model. To provide a better understanding of the involvement of PARP-1 in neuronal cell death associated with CNS diseases, further work to study the neuroprotective mechanisms and optimize the structures of these compounds is necessary. In addition, other possible protective mechanisms of these 2-aminothiazole analogues remain to be clarified, and this study provided confidence for the usefulness of the selected pharmacophore model to identify and design more potent PARP-1 inhibitors with diverse structures.

Experimental Section

Chemistry. Melting points were obtained on Taike X-5 microautomatic melting point detector and were uncorrected. Infrared absorption was detected on an impact 420 by FT-IR Spectrometer one scanning between 400 and 4000 cm^{-1}. ^{1}H NMR was recorded at 300 MHz on a PARIAN MERCURY VX-300 NMR. ^{13}C NMR was recorded at 100 MHZ on a Bruker AV400. And chemical shifts are reported in parts per million (ppm, δ) relative to tetramethyl-silane as an internal standard. Mass spectra were recorded on an Agilent 7890A15975C. Microwave reactor refitted from SanluoWP-650 household microwave oven (output power 650 W). The structures of all compounds were consistent with their spectral data. Unless otherwise noted, all materials were obtained from commercial suppliers and used without further purification, and the reported yields were not optimized.
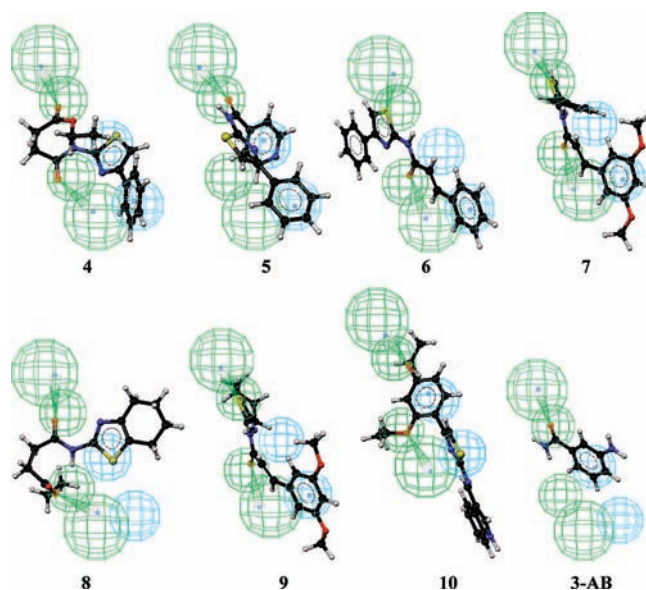

Figure 2. Mapping of designed compounds **4**−**10** and **3-AB** on the optimal pharmacophore developed against PARP-1. The green and blue contours represent the hydrogen bond accepting feature (HA) and hydrophobic aromatic feature (HPAR) respectively.
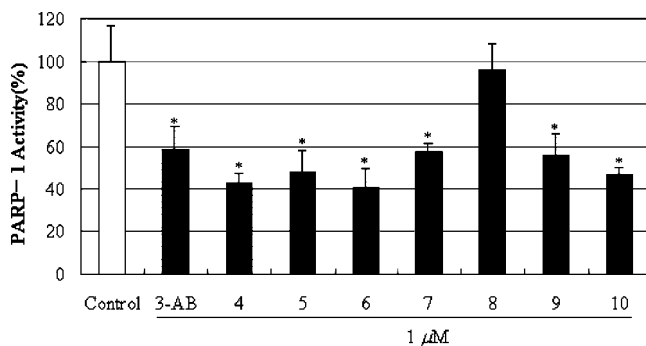
Figure 3. 2-Aminothiazole analogues inhibit PARP-1 activity at a concentration of 1 μM ($n = 3$ cultures) and the mean is presented. Signification difference from control group: "*", $P < 0.05$.

General Procedure 1. Preparation for 4,5-substituted-2-aminothiazole analogues. A mixture of acetophenone, thiourea, and iodine was stirred in microwave for a few minutes. The reaction mixture then was cooled, extracted with ether to remove ketone and iodine, and then dissolved in hot water. The solution was neutralized with Na$_2$CO$_3$, and recrystallized from alcohol.
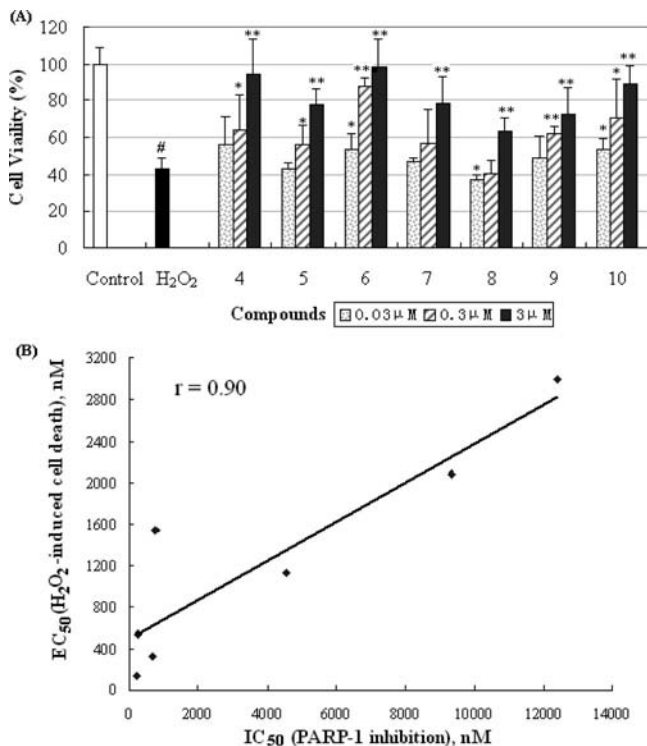
Figure 4. Cytoprotection by 2-aminothiazole analogues against H_2O_2-induced damage in PC12 cells and correlation with their PARP-1inhibitory potency. (A) Cell viability in each culture was quantified ($n = 10$ cultures), and the mean is presented. No toxicity was associated with the use of the designed compounds alone as assessed by MTT (data not shown). Signification difference from control group: "#", $P < 0.001$. Significant difference from H_2O_2 treated group: "*", $P < 0.05$ and "**", $P < 0.01$. (B) Positive correlation ($r = 0.90$) between the IC_{50} values of selected compounds for the inhibition of PARP-1 activity and their EC_{50} values for reduction of H_2O_2-induced cell death, P (that r is zero) < 0.0053.

4-Phenylthiazol-2-amine (1). Yield (63%); mp 149−151 °C (lit.[28] 146−148 °C). IR (KBr) σ/cm^{-1} 3446, 3437, 3255. ^{1}H NMR (CDCl$_3$) δ 5.11 (s,2H), 6.73 (s,1H), 7.28 (t, $J = 7.2$ Hz, 1H), 7.47 (t, $J = 7.2$ Hz, 2H), 7.78 (d, $J = 7.2$ Hz, 2H).

4,5,6,7-Tetrahydrobenzo[d]thiazol-2-amine (2). Yield (75%); mp 87−88 °C (lit.[29] 87−88 °C). IR (KBr) σ/cm^{-1} 3264, 3133, 1524. ^{1}H NMR (CDCl$_3$) δ 1.80 (s, 4H), 2.55 (s, 4H), 4.89 (s, 2H).

4-(2,4-Diethoxyphenyl)thiazol-2-amine (3). Yield (16%); mp 140−142 °C. ^{1}H NMR (CDCl$_3$) δ 1.32 (t, $J = 6.6$ Hz, 3H), 1.46 (t, $J = 6.6$ Hz, 3H), 4.11 (q, $J = 6.6$ Hz, 2H), 4.13 (q, $J = 6.6$ Hz, 2H), 5.94 (s, 2H), 6.45 (d, $J = 2.0$ Hz, 1H), 6.51 (dd, $J = 7.2$ Hz and $J = 2.0$ Hz, 1H), 6.73 (s, 1H), 7.63 (d, $J = 7.2$ Hz, 1H).

General Procedure 2. Synthesis of 4,5-substituted-2-aminothiazoles amide derivatives. 4,5-Substituted-2- aminothiazole (1 g) and acid or acyl chloride (1:1.2) were dissolved in 15 mL of acetone and then DMAP and DCC were added. The mixture was shaked continually at 25 °C for 24 h. The mixture was filtered, washed with 9 mL of acetone, and then the acetone solution was put together. Volatilized acetone and yielded the yellow solid. The solid was washed the by slightly distilled water and recrystallized with 75% alcohol.

Compounds **4−9** were prepared according to general procedure 2.

Ethyl 4-oxo-4-(4-phenylthiazol-2-ylamino) butanoate (4). Yield (44%); mp 168−169 °C. IR (KBr) σ/cm^{-1} 3431, 3273, 1720, 1689. ^{1}H NMR (CDCl$_3$) δ 1.25 (t, $J = 7.2$ Hz, 3H), 2.58 (t, $J = 6.6$ Hz, 2H), 2.68 (t, $J = 6.6$ Hz, 2H), 4.15 (q, $J = 7.2$ Hz, 2H), 7.14 (s, 1H), 7.33 (d, $J = 7.2$ Hz, 1H), 7.41 (dd, $J = 7.2$ Hz and $J = 7.5$ Hz, 2H), 7.82 (d, $J = 7.2$ Hz, 2H), 10.00 (s, 1H). ^{13}C NMR (CDCl$_3$)
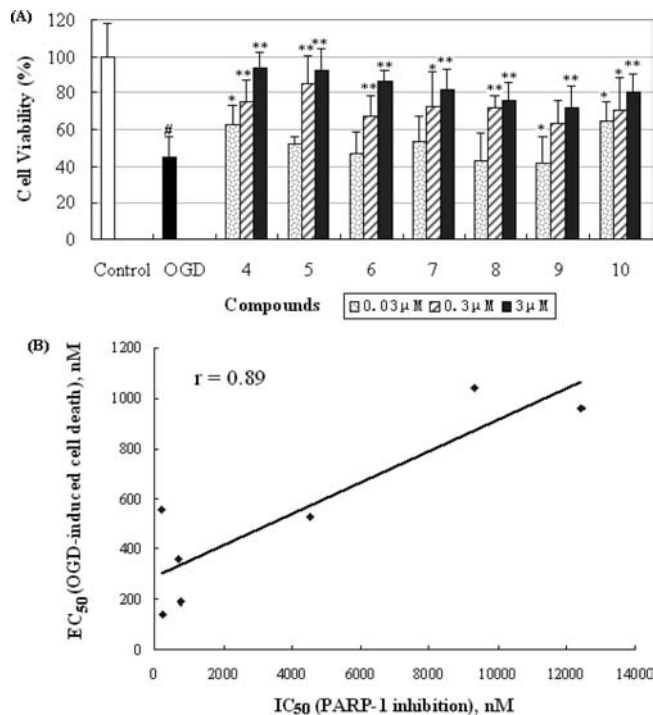
Figure 5. Cytoprotection by 2-aminothiazole analogues against OGD toxicity in PC12 cells and correlation with their PARP-1inhibitory potency. (A) Cell viability in each culture was quantified ($n = 10$ cultures), and the mean is presented. No toxicity was associated with the use of the designed compounds alone as assessed by MTT (data not shown). Signification difference from control group: "#", $P < 0.005$. Significant difference from OGD treated group: "*", $P < 0.05$ and "**", $P < 0.01$. (B) Positive correlation ($r = 0.89$) between the IC_{50} values of selected compounds for the inhibition of PARP-1 activity and their EC_{50} values for reduction of OGD -induced cell death, P (that r is zero) < 0.0072.
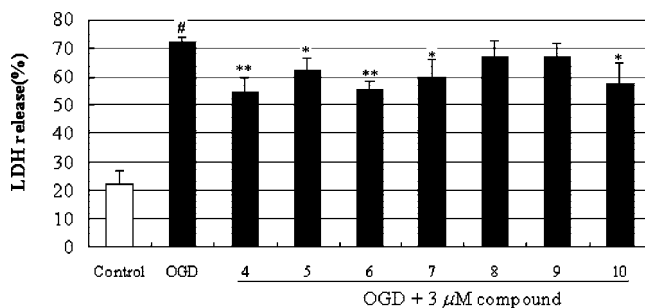

Figure 6. OGD-induced LDH release was attenuated by 3 μM 2-aminothiazole analogues in PC12 cells. Data are expressed as mean ± SD ($n = 4$ cultures). Signification difference from control group: "#", $P < 0.001$. Significant difference from OGD treated group: "*", $P < 0.05$; "**", $P < 0.001$.

δ 172.41, 169.37, 157.84, 149.47, 134.01, 128.82, 128.23, 126.13, 107.68, 61.10, 31.04, 29.03, 14.16. MS (ESI positive ion) m/z: 305.1 (M + 1).

N-(4-Phenylthiazol-2-yl)isonicotinamide (5). Yield (60%); mp 213−216 °C (lit. 206−208 °C). IR (KBr) σ/cm^{-1} 3400, 1602. ^{1}H NMR (CDCl$_3$) δ 7.23 (s, 1H), 7.25 (d, $J = 7.2$ Hz, 1H), 7.32 (t, $J = 7.2$ Hz, 2H), 7.58 (s, 2H), 7.67 (d, $J = 7.2$ Hz, 2H), 8.64 (s, 2H), 11.49 (s, 1H). ^{13}C NMR (CDCl$_3$) δ 163.52, 158.59, 150.72, 150.27, 139.07, 133.74, 128.85, 128.37, 126.10, 120.91, 108.61. MS (ESI positive ion) m/z: 282.2 (M + 1).

(E)-N-(4-Phenylthiazol-2-yl) cinnamamide (6). Yield (59%); mp 238−239 °C (lit. 225 °C). IR (KBr) σ/cm^{-1} 3393, 2929, 1630, 1533, 696. ^{1}H NMR (CDCl$_3$) δ 6.15 (d, $J = 15.0$ Hz, 1H), 7.26 (d, $J = 7.2$ Hz, 1H), 7.28 (s, 1H), 7.36−7.81 (m, 5H), 7.44 (t, $J = 7.2$ Hz,
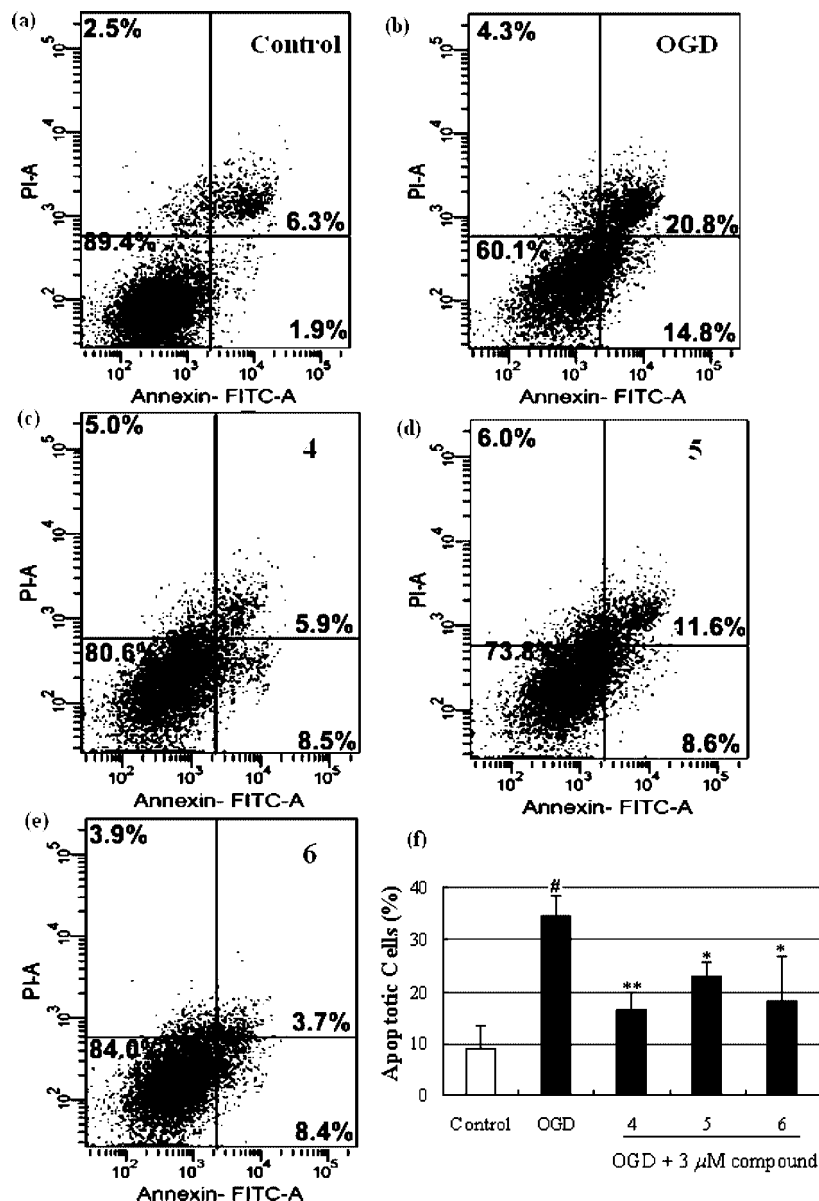
Figure 7. Compounds **4**−**6** significantly reduced apoptotic cells (early and late apoptotic cells) induced by OGD treatment ($n = 3$ cultures). (a−e) Dot plot for PC12 cells with Annexin/PI double stain. (a) control; (b) OGD (4 h and 18 h reoxygeneration); (c−e) OGD (4 h and 18 h reoxygeneration) + 3 μM compounds **4**−**6**, respectively. Shown are representative data from one of three independent experiments. (f) Data are expressed as the mean ± SD of results in three independent experiments. Significant difference from untreated control: "#", $P < 0.005$. Significant difference from OGD-treated model group: "*", $P < 0.05$; "**", $P < 0.005$.

2H), 7.88 (d, $J = 15.0$ Hz, 1H), 7.92 (d, $J = 7.2$ Hz, 2H), 11.63 (s, 1H). ^{13}C NMR (CDCl$_3$) δ 163.69, 159.79, 149.71, 144.53, 134.12, 133.93, 130.37, 128.99, 128.73, 128.50, 128.26, 126.18, 118.39, 108.42. MS (ESI positive ion) m/z: 307.1 (M + 1).

(*E*)-3-(3,5-Dimethoxyphenyl)-*N*-(4-phenylthiazol-2-yl)acrylamide (7). Yield (65%); mp 95−96 °C. IR (KBr) σ/cm^{-1} 3466, 3051, 1590, 1543. ^{1}H NMR (CDCl$_3$) δ 3.77 (s, 6H), 6.16 (d, $J = 15.0$ Hz, 1H), 6.35 (s, 2H), 6.45 (s, 1H), 7.22 (d, $J = 7.2$ Hz, 1H), 7.26 (s, 1H), 7.34 (t, $J = 7.2$ Hz, 2H), 7.61 (d, $J = 15.0$ Hz, 1H), 7.85 (d, $J = 7.2$ Hz, 2H), 11.63 (s, 1H). ^{13}C NMR (DMSO-d_6) δ 163.28, 160.73, 157.86, 149.05, 142.21, 136.20, 134.21, 128.64, 127.71, 125.60, 120.20, 108.41, 105.86, 102.15, 79.08, 55.94, 55.27. MS (ESI positive ion) m/z: 367.1 (M + 1).

Ethyl-4-oxo-5(4,5,6,7-tetrahydrobenzo[*d*]thiazol-2-ylamino)pentanoate (8). Yield (55%); mp 125−126 °C. IR (KBr) σ/cm^{-1} 3240, 3156, 2941, 1723, 1696, 1549, 1537. ^{1}H NMR (CDCl$_3$) δ 1.25 (t, $J = 6.9$ Hz, 3H), 1.84 (s, 4H), 2.65 (m, 2H), 2.69 (m, 2H), 2.73 (s, 4H), 4.15 (q, $J = 6.8$ Hz, 2H), 10.88 (s, 1H). ^{13}C NMR (DMSO-d_6) δ 171.98, 169.52, 154.60, 143.84, 120.97, 59.91, 29.73, 28.35, 25.97, 22.92, 22.60, 22.18, 14.02. MS (ESI positive ion) m/z: 283.2 (M + 1).

(*E*)-4-(3,5-Dimethoxyphenyl)-1-(4,5,6,7-tetrahydrobenzo[*d*]thiazol-2-ylamino)but-3-en-2-one (9). Yield (40%); mp 207−209 °C. IR (KBr) σ/cm^{-1} 3445, 2847, 1620, 1542. ^{1}H NMR (CDCl$_3$) δ 1.81 (s, 4H), 2.73 (s, 4H), 3.80 (s, 6H), 6.49 (s, 1H), 6.50 (d, $J = 15.0$ Hz, 1H), 7.62 (s, 2H), 7.68 (d, $J = 15.0$ Hz, 1H), 11.4 (s, 1H,). ^{13}C NMR (CDCl$_3$) δ 162.71, 160.55, 156.23, 143.34, 143.01, 135.61, 122.97, 118.88, 105.62, 102.03, 54.88, 25.78, 22.67, 22.36. MS (ESI positive ion) m/z: 345.1 (M + 1).

(*E*)-*N*-((1*H*-Indol-3-yl)methylene)-4-(2,4-diethoxyphenyl)thiazol-2-amine (10). Compound **3** (1.6 g, 6 nmol) and 1*H*-indole-3-carbaldehyde (0.9 g, 6 nmol) were dissolved in dehydrated alcohol (25 mL). Piperidine was added dropwise to the stirring solution, and the suspension was refluxed for 1 min by microwave at radiation power of 65 W and then for 1 h at radiation power of 130 W. Thereafter, the crude product was filtered off from the reaction mixture, washed with a small amount of distilled water, and

recrystallized from EtOH/Et$_2$O to give compound **10**. Yield (94%); mp 218−220 °C. IR (KBr) σ/cm^{-1} 3224, 3113, 1523.72, 1486.64. ^{1}H NMR (DMSO-d_6) δ 1.34 (t, $J = 6.6$ Hz, 3H), 1.48 (t, $J = 6.6$ Hz, 3H), 4.01 (q, $J = 6.6$ Hz, 2H), 4.10 (q, $J = 6.6$ Hz, 2H), 6.47 (d, $J = 2.4$ Hz, 1H), 6.48 (dd, $J = 7.2$ Hz and $J = 2.4$ Hz, 1H), 7.16−7.21 (m, 2H), 7.58 (d, $J = 7.2$ Hz, 1H), 7.68 (d, $J = 3.6$ Hz, 1H), 7.85 (d, $J = 7.2$ Hz, 1H), 8.15 (d, $J = 7.2$ Hz, 1H), 8.38 (d, $J = 3.6$ Hz, 1H), 9.10 (s, 1H), 11.64 (s, 1H). ^{13}C NMR (DMSO-d_6) δ 171.27, 164.70, 158.31, 156.20, 147.64, 136.52, 134.14, 129.73, 123.84, 122.37, 121.13, 120.62, 115.17, 113.67, 110.96, 104.21, 98.40, 62.74, 62.27, 13.77, 13.69. MS (ESI positive ion) *m/z*: 392.2 (M + 1).

Biology. PARP Universal Colorimetric Assay. PARP-1 inhibition was determined in a functional in vitro test using a PARP Universal Colorimetric Assay Kit (R&D catalogue no. 4677-096-K). This kit measures the incorporation of biotinylated poly(ADP-ribose) onto histone proteins in a 96-well histone-coated plate and tests the inhibition of PARP-1 activity. The test to screen PARP-1 inhibitors consists of the following steps: 15 μL/well human rPARP-HSA enzemy (0.5 unit/well, R&D 4668-050-01), 10 μL/well dilutions of PARP inhibitor (s), 2.5 μL/well 10 × activated DNA (R&D 4671-096-06), 2.5 μL/well 10 × PARP cocktail (contains biotinylated NAD$^+$, R&D 4671-096-03) and 20 μL/well 1 × PARP buffer (R&D 4671-096-02) were incubated on a 96-well histone-coated plate at room temperature for 1 h. After four washings with ice-cold PBS-T (PBS containing 0.05% Tween 20), 50 μL of diluted Strep-HRP (R&D 4800-30-06) was added to each well and the plate was incubated at room temperature for 1 h. After four washings with PBS-T, 50 μL of TACS-Sapphire (R&D 4822-96-08) was added to each well and the plate was incubated for 15−30 min in the dark. TACS-Sapphire is a horseradish-peroxidase (HRP) substrate generating a soluble blue color. Then 50 μL of 0.2 N HCl per well was added to stop this reaction. Then the plate can be read at 450 nm with a microplate reader. The positive control, 3-aminobenzamide, was provided by this kit (4667-50-03). All of the compounds were freshly prepared as stock solution with dimethyl sulfoxide (DMSO) and diluted with the PARP buffer. The final concentration of DMSO in the assay was less than 0.5%, and the same concentration of DMSO in PARP buffer was used as a control in this experiment.

Cell Culture. Rat PC12 cells were obtained from Chinese Type Culture Collection and have been differentiated to be neuron-like by treating with nerve growth factor (NGF). We have used these PC12 cells as a cell culture model for screening novel neuroprotective agents. Some nature polyphenolic compounds in our previous study, which have showed protective effects in oxidant stress induced PC12 cell injury, such as breviscapine and tetrahydroxystilbene glucoside, also exhibited neuroprotection in MCAO or 2VO animal models. Cultures of PC12 cells were maintained in DMEM containing 5% heat-inactivated fetal calf serum, 10% heat-inactivated horse serum, 100 U/mL penicillin, and 100 μg/mL streptomycin in a humidified atmosphere of 95% air and 5% CO$_2$ at 37 °C. The culture medium was changed and the cells were passaged by trypsinization every 3 to 4 days.

OGD-Induced Cell Death in PC12 Cell Cultures. Cells (4 × 10^4 cells/200 μL) were seeded into 96- or 6-well plates and then incubated in a humidified atmosphere of 95% air and 5% CO$_2$ at 37 °C for 2 days. To induce OGD stress, the cell culture medium was removed and the cells were washed twice with a glucose-free isotonic salt solution (OGD buffer pH 7.4) consisting of the following in mM: 20 NaHCO$_3$, 120 NaCl, 5.36 KCl, 0.33 Na$_2$HPO$_4$, 0.44 KH$_2$PO$_4$, 1.27 CaCl$_2$, and 0.81 MgSO$_4$ and incubated in the same volume OGD buffer.[31] Cells were then incubated at 37 °C in an oxygen-free incubator (95% N$_2$ and 5% CO$_2$) for 4 h (OGD). As a control for OGD, PC12 cells were incubated in OGD buffer supplemented with 5% bovine calf serum, 10% horse serum, and 4.5 mg/mL glucose in normoxic conditions for the indicated length of time. At the end of the OGD period, the medium was replaced with culture medium for the indicated time, and the cultures were put back in the incubator for an additional 18 h at the regular atmospheric oxygen level (reoxygenation). When required compounds (3, 0.3 and 0.03 μM) were added to the OGD buffer and the reoxygenation culture, all of the compounds were freshly prepared as stock solution with dimethyl sulfoxide (DMSO) and diluted with OGD buffer or DMEM. Less than 0.5% DMSO has no protective or toxic effects when used alone.

H$_2$O$_2$-Induced Cell Death in PC12 Cell Cultures. Cells (4 × 10^4 cells/200 μL) were seeded into 96- well plates and then incubated in a humidified atmosphere of 95% air and 5% CO$_2$ at 37 °C for 2 days. In the experiment, the cells in DMEM were exposed to different compounds (3, 0.3 and 0.03 μM) for 2 h at 37 °C. Then H$_2$O$_2$ was added to the cells at a final concentration of 550 μM. The plates were further incubated at 37 °C for 6 h.

MTT Assay. After various treatments, cell viability was measured by using the MTT assay, which is based on the conversion of MTT to formazan crystals by mitochondrial dehydrogenases. In live cells, mitochondrial enzymes have the capacity to transform MTT into insoluble formazan. Cell cultures were incubated with MTT solution (5 mg/mL) for 4 h at 37 °C. Following this, the medium was discarded and DMSO was added to solubilize the reaction product formazan by shaking for 15 min. Absorbance at 492 nm was measured with a microplate reader (ELx800, Bio-Tek, Winooski, VT). Cell viability of vehicle-treated control group not exposed to either H$_2$O$_2$ or OGD was defined as 100%. Cell viability was expressed as a percentage of the value in control cultures.

LDH assay. The LDH activity assay was performed according to the protocols of a LDH kit. To confirm the cell death, the amount of LDH released to the medium and total LDH were determined 18 h after OGD. Briefly, an aliquot of the culture supernatants (extracellular) or cell dissociation solution (intracellular) was mixed with nicotinamide adenine dinucleotide (NAD) and lactate solution. Colorimetric absorbance was measured at 490 nm with a microplate reader, respectively. Total LDH activity was calculated by adding the values for extracellular and intracellular LDH that were measured in live cells treated with 1% Triton X-100. The ratio of released LDH (extracellular) versus total LDH (extracellular + intracellular) was calculated and expressed as a percentage of total LDH.

Assessment of Apoptosis. Flow cytometry was used to assess the membrane and nuclear events during apoptosis. The assay was performed with a two color analysis of FITC-labeled Annexin V binding and PI uptake using the Annexin V-FITC apoptosis detection kit. Briefly, after reoxygenation, apoptotic cells were harvested by centrifugation of culture medium at 1000 rpm for 10 min, whereas adherent cells were trypsinized and subsequently collected by centrifugation. The cells were washed with PBS and resuspended in 1 mL of binding buffer. An aliquot of 100 μL was incubated with 5 μL of Annexin V-FITC and 10 μL of PI for 15 min in dark at room temperature and 400 μL of PBS was added to each sample. The FITC and PI fluorescence were measured through a FL-1 filter (530 nm) and a FL-2 filter (585 nm), respectively, on BD-LSR flow cytometer using Cell Quest software. Positioning of quadrants on Annexin V/PI dot plots was performed and live cells (Annexin V−/PI−, represent in the lower left quadrants of the cytograms), early/primary apoptotic cells (Annexin V+/PI−, represent in the lower right quadrants), and late/secondary apoptotic cells (Annexin V+/PI+, represent in the upper right quadrants) were distinguished.[32] The upper left quadrants represent cells damaged during the procedure.

Statistical Analysis. Data were expressed as means ± SD. Comparison between two groups were evaluated by the unpaired Student's *t* test. Differences were considered significant at $P < 0.05$.

Supporting Information Available: Details on pharmacophore modeling and chromatographic analytical data for determining

degree of purity for target compounds **4−10**. This material is available free of charge via the Internet at http://pubs.acs.org.

References

(1) Nguewa, P. A.; Fuertes, M. A.; Valladares, B.; Alonso, C.; Perez, J. M. Poly(ADP-ribose) polymerases: Homology, structural domains and functions. Novel therapeutical applications. *Prog. Biophys. Mol. Biol.* **2005**, *88*, 143–172.

(2) Ame, J. C.; Spenlehauer, C.; Murcia, G. The PARP superfamily. *Bioessays* **2004**, *26*, 882–893.

(3) Tentori, L.; Portarena, I.; Graziani, G. Potential clinical applications of poly(ADP-ribose) polymerase (PARP) inhibitors. *Pharmacol. Res.* **2002**, *45*, 73–85.

(4) Ha, H. C.; Snyder, S. H. Poly(ADP-ribose) polymerase is a mediator of necrotic cell death by depletion. *Proc. Natl. Acad. Sci. U.S.A.* **1999**, *96*, 13978–13982.

(5) Oliver, F. J.; Murcia, C. N.; Nacci, C.; Decker, P.; Andriantsitohaina, R.; Muller, S.; Rubia, G.; Stoclet, J. C.; Murcia, G. Resistance to endotoxic shock as a consequence of defective NF-KB activation in poly(ADP-ribose) polymerase-1 deficient mice. *EMBO J.* **1999**, *18*, 4446–4454.

(6) Mandir, A. S.; Poitras, M. F.; Berliner, A. R.; Herring, W. J.; Guastella, D. B.; Feldman, A.; Poirier, G. G.; Wang, Z. Q.; Dawson, T. M.; Dawson, V. L. NMDA but not non-NMDA excitotoxicity is mediated by poly(ADP-ribose) polymerase. *Neuroscience* **2000**, *20*, 8005–8011.

(7) Pieper, A. A.; Wallws, T.; Wei, G.; Clements, E. E.; Verma, A.; Snyder, S. H.; Zweier, J. L. Myocardial postischemic injury is reduced by poly(ADP-ribose) polymerase-1 gene disruption. *Mol. Med.* **2000**, *6*, 271–282.

(8) Yu, S. W.; Wang, H.; Poitras, C. C.; Bowers, W. J.; Federoff, H. J.; Poirier, G. G.; Dawson, T. M.; Dawson, V. L. Mediation of poly(ADP-ribose) polymerase-1-dependent cell death by apoptosis-inducing factor. *Science* **2002**, *297*, 259–263.

(9) Kauppinen, T. M.; Swanson, R. A. The role of poly(ADP-ribose) polymerase-1 in CNS disease. *Neuroscience.* **2007**, *145*, 1267–1272.

(10) Ferraris, D.; Ficco, R. P.; Dain, D.; Ginski, M.; Lautar, S.; Wisdom, K. L.; Liang, S.; Lin, Q.; Lu, M. X. C.; Morgan, L.; Thomas, B.; Williams, L. R.; Zhang, J; Zhou, Y.; Kalish, V. J. Design and synthesis of poly(ADP-ribose) polymerase-1 (PARP-1) inhibitors. Part 4: Biological evaluation of imidazobenzodiazepines as potent PARP-1 inhibitors for treatment of ischemic injuries. *Bioorg. Med. Chem.* **2003**, *11*, 3695–3707.

(11) Iwashita, A.; Hattori, K.; Yamamoto, H.; Ishida, J.; Kido, Y.; Kamijo, K.; Murano, k.; Miyake, H.; Kinoshita, T.; Warizaya, M.; Ohkubo, M.; Matsuoka, N.; Mutoh, S. Discovery of quinazolinone and quinoxaline derivatives as potent and selective poly(ADP-ribose) polymerase-1/2 inhibitors. *FEBS Lett.* **2005**, *579*, 1389–1393.

(12) Steinhagen, H.; Gerisch, M.; Mittendorf, J.; Schlemmer, K. H.; Albrecht, B. Subtituted uracil derivatives as potent inhibitors of poly(ADP-ribose) polymerase-1 (PARP-1). *Bioorg. Med. Chem. Lett.* **2002**, *12*, 3187–3190.

(13) Jagtap, P. G.; Southan, G. J.; Baloglu, E.; Ram, S.; Mabley, J. G.; Marton, A.; Salzman, A.; Szabo, C. The discovery and sythesis of novel adenosine substituted 2, 3-dihydro-1*H*-isoindol-1-ones: Potent inhibitors of poly(ADP-ribose) polymerase-1 (PARP-1). *Bioorg. Med. Chem. Lett.* **2004**, *14*, 81–85.

(14) Loh, V. M.; Cockcroft, X. L.; Dillon, K. J.; Dixon, L.; Drzewiecki, J.; Eversley, P. J.; Gomez, S.; Hoare, J.; Kerrigan, F.; Matthews, L. T. W.; Menear, K. A.; martin, N. M. B.; Newton, R. F.; Paul, J.; Smith, G. C. M.; Vile, J.; whittle, A. J. Phthalazinones. Part 1: The design and synthesis of a novel series of potent inhibitors of poly(ADP-ribose) polymerase. *Bioorg. Med. Chem. Lett.* **2005**, *15*, 2235–2238.

(15) Ferraris, D.; Ko, Y. S.; Phhuski, T.; Ficco, R. P.; Serdyuk, L.; Alemu, C.; Bradford, C.; Chiou, T.; Hoover, R.; Huang, S.; Lautar, S.; Liang, S.; lin, Q.; Lu, M. X. C.; Mooney, M.; Morgan, L.; Qian, Y.; Tran, S.; Williams, L. R.; Wu, Y. Q.; Zhang, J.; Zou, Y.; Kalish, V. Design and synthesis of poly ADP-ribose polymerase-1 inhibitors. 2. Biological evaluation of aza-5[*H*]-phenanthridin-6-ones as potent, aqueous-

(16) Ferraris, D.; Ficco, R. P.; Pahutski, T.; Lautar, S.; Huang, S.; Zhang, J.; Kalish, V. Design and synthesis of poly(ADP-ribose) polymerase-1 (PARP-1) inhibitors. Part 3: In vitro evalution of 1,3,4,5-tetrahydro-benzo[*c*][1,6]- and [*c*][1,7]-naphthyridin-6-ones. *Bioorg. Med. Chem. Lett.* **2003**, *13*, 2513–2518.

(17) Kurogi, Y.; Guner, O. F. Pharmacophore modeling and three-dimensional database searching for drug design using catalyst. *Curr. Med. Chem.* **2001**, *8*, 1035–1055.

(18) Debnath, A. K. Pharmacophore mapping of a series of 2,4-diamino-5-deazapteridine inhibitors of *Mycobacterium avium* comples dihydrofolate reductase. *J. Med. Chem.* **2002**, *45*, 41–53.

(19) Kurogi, Y.; Miyata, K.; Okamura, T.; Hashimoto, K.; Tsusumi, K.; Nasu, M.; Moriyasu, M. Discovery of novel mesangial cell proliferation inhibitors using a three-dimensional database searching method. *J. Med. Chem.* **2001**, *44*, 2304–2307.

(20) Kaminski, J. J.; Rane, D. F.; Snow, M. E.; Weber, L.; Rothofsky, M. L.; Anderson, S. D.; Lin, S. L. Identification of novel farnesyl protein transferase inhibitors using three-dimensional database searching methods. *J. Med. Chem.* **1997**, *40*, 4103–4112.

(21) Zhang, W. T.; Yan, H.; Jiang, F. C. Construction of pharmacophore model of PARP-1 inhibitor. *Yao Xue Xue Bao.* **2007**, *42*, 279–285; Chinese.

(22) Ruf, A.; Murcia, G.; Schulz, G. E. Inhibition and NAD$^+$ binding to poly(ADP-ribose) polymerase as derived from crystal structures and homology modeling. *Biochemistry* **1998**, *37*, 3893–3900.

(23) Costantino, G.; Macchiarulo, A.; Camaioni, E.; Pellicciari, R. Modeling of poly(ADP-ribose) polymerase (PARP) inhibitors. Docking of ligands and quantitative structure-activity relationship analysis. *J. Med. Chem.* **2001**, *44*, 3786–3794.

(24) Geronikaki, A.; Dearden, J. C.; Filimonov, D.; Galaeva, I.; Garibova, T. L.; Gloriozova, T.; Krajneva, V.; Lagunin, A.; Macaev, F. Z.; Molodavkin, G.; Poroikov, V. V.; Pogrebnoi, S. I.; Shepeli, F.; Voronina, T. A.; Tsitlakidou, M.; Vlad, L. Design of new congnition enhancers: From computer prediction to synthesis and biological evalution. *J. Med. Chem.* **2004**, *47*, 2870–2876.

(25) Schneider, C. S.; Mierau, J. Dopamine autoreceptor agonist: Resolution and pharmacological activity of 2,6-diaminotetrahydrobenzothiazole and an aminothiazole analog of apomorphine. *J. Med. Chem.* **1987**, *30*, 494–498.

(26) Kin, K. M.; Kim, K. H.; Kang, T. C.; Kim, W. Y.; Lee, M.; Jung, H. J.; Hwang, I. K.; Ko, S. B.; Koh, J. Y.; Won, M. H.; Oh, E.; Shin, I. Design and biological evaluation of novel antioxidants containing *N-t*-butyl-*N*-hydroxylaminophenyl moieties. *Bioorg. Med. Chem. Lett.* **2003**, *13*, 2273–3375.

(27) Zhu, X.; Yu, Q. S.; Cutler, R. G.; Culmsee, C. W.; Holloway, H. W.; Lahiri, D. K.; Mattson, M. P.; Greig, N. H. Novel p53 inactivators with neuroprotective action: Syntheses and pharmacological evaluation of 2-imino-2,3,4,5,6,7-hexahydrobenzothiazole and 2-imino-2,3,4,5,6,7-hexahydrobenzoxazole derivatives. *J. Med. Chem.* **2002**, *45*, 5090–5097.

(28) King, L. C.; Miller, F. M. The reaction of diazoketones with thioamide derivatives. *J. Am. Chem. Soc.* **1949**, *71*, 367–368.

(29) King, L. C.; Hlavacek, R. J. The reaction of ketones with iodine and thiourea. *J. Am. Chem. Soc.* **1950**, *72*, 3722–3725.

(30) Lo, E. N.; Prince, B. H.; Wei, M.; Panahian, N. Inhibition of poly(ADP-ribose) polymerase: Reduction of ischemic injury and attenuation of *N*-methyl-D-aspartate-induced neurotransmitter dysregulation. *Stroke.* **1998**, *29*, 830–836.

(31) Lenart, B.; Kintner, D. B.; Shull, G. E.; Sun, D. Na-K-Cl cotransporter-mediated intracellular Na$^+$ accumulation affects Ca^{2+} signaling in astrocytes in an in vitro ischemic model. *Neurobiol. Dis.* **2004**, *24*, 9585–9597.

(32) Vermes, I.; Haanen, C.; Nakken, H. S.; Reutelingsperger, C. A novel assay for apoptosis flow cytometric detection of phosphatidylserine expression on early apoptotic cells using fluorescein iabelled annexin V. *J. Immunol. Methods* **1995**, *184*, 39–51.